SIMULATING THE FRICTION SOUNDS USING A FRICTION-BASED ADHESION THEORY MODEL

Takayuki Nakatsuka

Department of Pure and Applied Physics,
Waseda University
Tokyo, Japan
t59nakatsuka@fuji.waseda.jp

Shigeo Morishima

Waseda Research Institute for Science and Engineering
Tokyo, Japan
shigeo@waseda.jp

ABSTRACT

Synthesizing a friction sound of deformable objects by a computer is challenging. We propose a novel physics-based approach to synthesize friction sounds based on dynamics simulation. In this work, we calculate the elastic deformation of an object surface when the object comes in contact with other objects. The principle of our method is to divide an object surface into microrectangles. The deformation of each microrectangle is set using two assumptions: the size of a microrectangle (1) changes by contacting other object and (2) obeys a normal distribution. We consider the sound pressure distribution and its space spread, consisting of vibrations of all microrectangles, to synthesize a friction sound at an observation point. We express the global motions of an object by position based dynamics where we add an adhesion constraint. Our proposed method enables the generation of friction sounds of objects in different materials by regulating the initial value of microrectangular parameters.

1. INTRODUCTION

Friction and its sound are familiar phenomena. We encounter such sounds almost constantly in our daily lives: sounds from brushing of hand bags and garments, footsteps, rustling of leaves, and rolling of tires are some examples of friction sounds. The sounds in computer animations (movies, video games, etc.) are created by Foley artists. Foley artists use two approaches to produce sound effects: recording actual but not actual sounds (a conspicuous example is rolling adzuki beans on a basket to create a sound of waves) and using a synthesizer to compose sounds. However, creation of sound effects by these approaches places a heavy burden on Foley artists to create various ingenious plans to create ideal sounds. On the other hand, friction is a complicated phenomenon on a macroscale as well as a microscale and physical parameters vary for each material. Also, extracting the theoretical principle of friction using numerical calculation is challenging. Simulating its sound is then difficult without considering multi-scale of the material.

In this paper, we suggest novel techniques to synthesize friction sounds based on physics simulation. Our proposed method has wide applicability and can create sounds of various objects from rigid to elastic. In related works, objects are limited to only rigid materials [1, 2] or databases constructed by recorded friction sounds are used [3–5]. Our method adopts a manner of subsuming the adhesion theory [6] into computer animation and uses position based dynamics (PBD) [7] framework, which is widely accepted in the field of computer animation because of its robustness and simplicity for simulation.

2. RELATED WORK

On a microscale, an object surface is usually rough with asperities which is composed of a mass of atoms and molecules. Each asperity forms an elevation irregularly on a surface. Therefore, we consider the irregularities of the actual contact point positions formed by the distribution of asperities. The computation of friction at the actual contact point on the object surface is modeled by direct numerical solution [8,9] and a method specialized in computation [10]. However, some aspects of friction need further understanding to model them exactly. Because a precise friction model is not available at present, prediction of friction sounds that are sensitive to friction parameters is fraught with errors. Avanzini et al. [11] and Desvages et al. [12] focused on friction in a bowed string. Akay et al. [13] have compiled past studies about friction sounds. These studies explain the cause of friction sounds in great detail for different target bodies. In this paper, we suggest a friction model which has a wide application.

In regard to computer animation, Takala et al. [14] and Gaver [15] suggested a series of frameworks to express a sound (sound rendering) for the first time. The series of frameworks of sound rendering synthesize the sound according to the motion of objects and compute a spread of the sound. Based on these frameworks, Van den Doel and Pai [16, 17] generated a plausible sound of objects by performing linear modal analysis of the input shape. Those studies were the first to apply computer mechanics to sound synthesis but they could handle only simple shapes. Other approaches synthesize the sound of specific musical instruments [18–21]. O'Brien et al. [22, 23] and Van den Doel et al. [1] proposed a solution that can be generalized to all rigid objects. These works made it possible to put knowledge to practical use. As a pioneering work in virtual reality of sounds, Pai et al. [24] built an interactive system to generate sounds synthesized based on the motion of the user at the time of contact to the material body [25–27]. In addition, several works have reported synthesis of sounds of collision or contact with objects based on linear modal analysis and speed-up and optimization of such synthesis [28–35]. It is difficult to adopt the linear modal model to thin-shell objects where a nonlinearity exists, but Chadwick et al. [34], Bilbao [20] and Cirio et al. [36] have suggested improved techniques to generate high-quality sounds in such cases. Most of these studies aimed at rigid bodies and provided outputs that are plausible sounds of "rolling friction" or "sticking collisions," which are modeled by friction models [37, 38], but not of "sliding friction," which is caused by sliding objects. The reason these techniques are not good at synthesizing the sounds of sliding friction is that sliding friction involves continuous collisions in contrast with rolling friction, which involves discrete collisions.

Van den Doel et al. [1] generated friction sounds to remark on the fractal characteristics of asperities. However, the model is applicable only to simple and homogeneous shapes of material body. Ren at al. [2] synthesized friction sounds using the techniques of Raghuvanshi et al. [28] and a surface model of the object in three phases of scales following [1]. However, the model could not treat objects with nonlinear properties such as deformation of clothes. On the other hand, An et al. [3] made friction sounds synthesized to the cloth animation using a database of recorded actual sounds. The velocity of the cloth mesh top is matched with entries in the database and the corresponding fragment of friction sound is returned, and the fragments are joined to synthesize the sound. Making of such a database requires a large amount of time and labor to record the sounds of rubbing clothes at various speeds. Our proposed method solves these problems partially with a novel surface model using a physically well-grounded simulation and enables synthesis of friction sounds for deformable objects.

3. BACKGROUND

3.1. Principle of Friction

Friction is a complicated phenomenon to solve analytically because it is an irreproducible, microscale phenomenon (an object surface slightly deforms by friction). As shown in Fig. 1, when an external force is applied on an object in contact with another object in order to move the first object, friction acts to impede the motion. The force caused by friction is called friction force. The magnitude of friction force depends on the objects in contact.

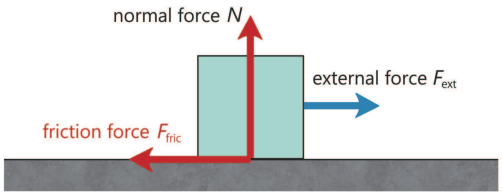

Figure 1: *Forces during motion of two objects in contact. The friction force F_{fric} is the resistance between the relative motion of the two bodies.*

The classical laws of friction derived from observing objects, known as Amonton-Coulomb laws of friction, are as follows.

- Amonton's first law: magnitude of friction force is independent of contact area.
- Amonton's second law: magnitude of friction force is proportional to magnitude of normal force.
- Coulomb's law of friction: magnitude of kinetic friction is independent of speed of slippage.

A phenomenological discussion of Amonton-Coulomb laws is incorporated in the theory of adhesion [6], which is deeply rooted in the field of tribology. Adhesion theory describes a friction phenomenon based on Amonton-Coulomb model of friction, especially with a focus on the second property. The main principle of adhesion theory is that the contact between two object is present at points. The surface roughness of an object is on a sufficiently small scale. In particular, the convex portion of the object surface is termed as an asperity. Friction is considered to be caused by contact between asperities of the two objects (called actual contact points). At each actual contact point, there is adhesion (or bond) of two objects due to the interaction between molecules or atoms of the object surface. The sum of the areas of the actual contact points is called actual contact area. The force required to overcome the adhesion at actual contact points is the friction force, which is represented by the following equation:

$$F_{fric} = \sigma_s \times A_r \tag{1}$$

where F_{fric} is the friction force, σ_s is the shear strength, and A_r is the actual contact area. Assuming A_r is related to the load W as $A_r = aW$ with a constant of proportionality a, the friction coefficient μ is given by the following equation.

$$\mu = \frac{F_{fric}}{W} = \frac{\sigma_s \times A_s}{W} = a\sigma_s \tag{2}$$

Therefore, the friction coefficient μ does not depend on the apparent area of contact (Amonton's first law of friction). An actual contact point is formed at the point surrounded by the green rectangle in Fig. 2, forming a "stick" state. The adhesion at the pair of asperities is cut by the elastic energy and the actual contact point collapses a few moments later, termed as a "slip" state, when the two objects move against each other in a horizontal direction. The energy dissipated in this series of processes is equal to the work done by the friction force. The stick-slip phenomenon is repetition of the process of adhesion and cutting the pair of asperities. The global motion of the object and the stick-slip phenomenon at actual contact points are not related. The actual contact points change with time by the motion of the object. Even though the object continues the sliding movement at a regular velocity, asperities on the object surface are in stick state with pairs of asperities on the different object surfaces forming the actual contact points. An asperity in the stick state is deformed by the motion of an object, and the elastic energy is accumulated around the asperity. The actual contact point beyond the limit of elasticity slip by the elastic energy and the neighborhood of an asperity vibrate around the equilibrium state. The stick-slip motion is repeated locally within the system during the movement of an object at a constant velocity. Since the frequency of local slip per unit time is proportional to the sliding velocity, the energy dissipation per unit time is also proportional to the sliding velocity. Therefore, the friction force does not depend on the sliding velocity as the energy dissipation per unit time is equal to the friction force times the sliding velocity. Such a localized stick-slip motion explains the third Amonton-Coulomb law.

3.2. Sound Propagation

The sound propagates in air as a wave. In general, a sound propagated through the space Ω can express using a wave equation (3):

$$\nabla^2\phi(\vec{x},t) - \frac{1}{c^2}\frac{\partial^2\phi(\vec{x},t)}{\partial t^2} = 0, \quad \vec{x} \in \Omega \tag{3}$$

where c is the speed of sound in air (at standard temperature and pressure, it is empirically described as $c = 331.5 + 0.6t$ [m/s] with temperature t [°C]). In the study of acoustics, acoustic pressure $p(\vec{x},t)$ and particle velocity $\mathbf{u}(\vec{x},t)$ are used as a variable of the wave equation as follows.

$$\left(\nabla^2 - \frac{1}{c^2}\frac{\partial^2}{\partial t^2}\right) p(\vec{x},t) = 0 \tag{4}$$

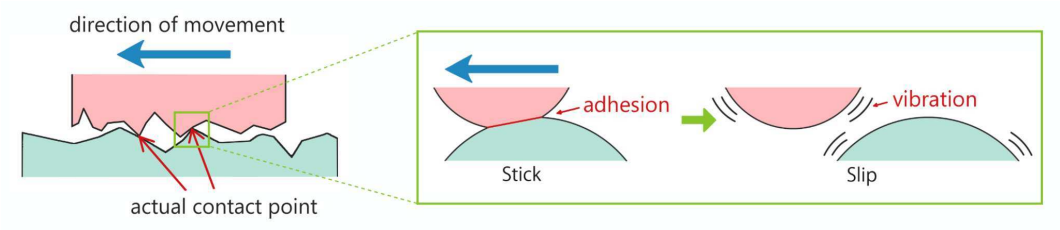

Figure 2: *Illustration of contact between two objects and the stick-slip phenomenon at an actual contact point. Due to the roughness of the surface, objects are in contact with each other at points, instead of a large area.*

$$\left(\nabla^2 - \frac{1}{c^2}\frac{\partial^2}{\partial t^2}\right)\mathbf{u}(\vec{x},t) = 0 \tag{5}$$

The relation between acoustic pressure and particle velocity is described as first-order partial differential equation (PDE):

$$\rho\frac{\partial \mathbf{u}(\vec{x},t)}{\partial t} = -\nabla p(\vec{x},t) \tag{6}$$

where ρ is the density of the air (at standard temperature and pressure, it is empirically described as $\rho = 1.293/(1 + 0.00367t)$ [kg/m^3] with temperature t [°C]).

4. GENERATE FRICTION SOUND

Our physics-based method comprises three steps (see Fig. 3). First, we separate an object surface into microrectangles (local shape) around each vertex of the object and define their initial size. The initial size of the microrectangles is decided by the object texture (e.g., in the case of a cloth, the initial size is the thread diameter) and is deformed on the basis of two assumptions: the deformation (1) depends on the velocity of the contacting vertex and (2) the initial size obeys normal distributions. The deformation of a microrectangle is given by the following equation:

$$D\nabla^4 w + \rho\frac{\partial^2 w}{\partial t^2} = 0 \tag{7}$$

where D is the flexural rigidity, w is the displacement, and ρ is the density of the object [39]. We then determine the global shape of the object using PBD [7]. As constraints, we adopt a distance constraint between the vertices of the object and an adhesion constraint between two objects. Finally, we synthesize the sounds generated by each microrectangle at the observation point by using a wave equation [40]. The synthesized sound can be expressed as a linear sum of sounds because the sound waves are independent.

4.1. Determination of Vibration Area

The spectrum of friction sound depends on the velocity of the object. Therefore, An et al. [3] recorded several friction sounds at different speeds and made a friction sound database consisting of pairs of a sound spectrum and a velocity. We also conducted experiments to record friction sounds as described in their method [3] and confirmed the relation between spectrum and velocity (see Fig. 4). To reflect the dependence on velocities of the object, we define relationships between sides a and b of the rectangular domain and the velocity v of an actual contact point as follows:

$$\frac{1}{a} = \alpha v, \quad \frac{1}{b} = \beta v \tag{8}$$

where α and β are constants. The roughness of the object surface is expressed as dispersions σ_a and σ_b, respectively, of the normal distributions of lengths of a and b.

4.2. Determination of Global Shape and Amplitude

Several studies have used elastic body simulation for computer animation. There are three main methods used in computer graphics. Finite element method (FEM) is the one of most popular methods and is based on physics. The spring mass model [41] sacrifices accuracy to achieve a low costs of computation. In addition, there is a specialized technique for computer animation [42]. To determine the global transition of the body shape and the amplitude which of vibration of the rectangular domains by friction, we handle the mesh vertices of the material body as true actual contact points and control their positions. This is because PBD is widely known in the field of computer graphics and has the advantages of robustness and simplicity. Let us postulate there are N particles with positions $\mathbf{x}_i$ and inverse masses $g_i = 1/m_i$. For a constraint C, the positional corrections $\Delta\mathbf{q}_i$ is calculated as

$$\Delta\mathbf{q}_i = -sg_i\nabla_{\mathbf{q}_i}C(\mathbf{q}_1,\cdots,\mathbf{q}_n) \tag{9}$$

where

$$s = \frac{C(\mathbf{q}_1,\cdots,\mathbf{q}_n)}{\sum_j g_j\nabla_{\mathbf{q}_i}C(\mathbf{q}_1,\cdots,\mathbf{q}_n)}. \tag{10}$$

As constraints with respect to the position of the object vertices, we adapt constraints representing the shape deformation of the body and the adhesion at actual contact points: the respective terms defined as $C_{Deformation}$ and $C_{Adhesion}$. Then, the total constraint C is expressed by

$$C = C_{Deformation} + C_{Adhesion}. \tag{11}$$

In our method, we adopt a distance constraint between the vertices of the body for $C_{Deformation}$ and a relational expression for $C_{Adhesion}$, which is given as

$$C_{Adhesion} = \begin{cases} \frac{Z}{r} & (r > d) \\ Z & (r \le d) \end{cases}. \tag{12}$$

where r is the distance between a vertex of the object and another object, Z is the adhesion degree depended on material properties and d is the effective distance of the adhesion. Equation (12) denotes represents the fact that the attracting forces between the objects are given as a Coulomb potential. Then, the amplitude A of the rectangular amplitude is determined by the following equation:

$$A = \frac{1}{\sharp X}\left(\mathbf{x}_i(t+\Delta t) - \mathbf{x}_i(t)\right) \tag{13}$$

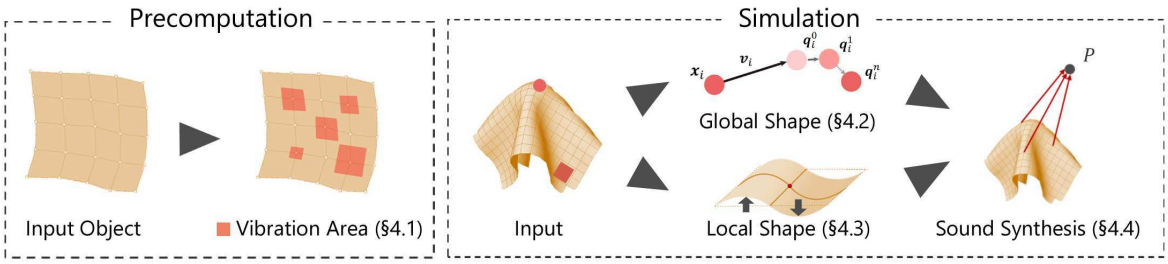

Figure 3: ***Overview:*** *For the input object, we first define the vibration area which deform independently with regard to each surrounding vertex of the object surface. We then compute a global shape of the object and an amplitude of each vibration area to use PBD, and a local shape of each rectangle. Finally, we synthesize the sounds which is generated by each surrounding vertex of the object at the observation point P based on wave equation.*

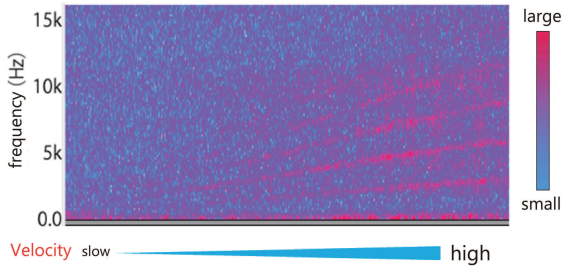

Figure 4: *A sound spectrogram of the friction sounds of cupra fiber. The red parts of the figure show that spectrum and velocity are related.*

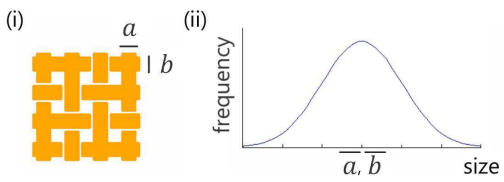

Figure 5: *An example of setting initial parameters of a and b. In the case of a cloth, we use the diameter of the cloth's string and a normal distribution of their sizes.*

where $\mathbf{x}_i(t)$ is the i-th vertex position of the object at time t and X is the direct product of the sets M and N defined as

$$M = \{m \mid m = 2k + 1\} \tag{14}$$
$$N = \{n \mid n = 2l + 1\} \tag{15}$$

where m and n are the mode orders of the vibration and k and l are natural numbers $\mathbf{N} \cup \{0\}$.

4.3. Determination of Local Shape

This section describes the main principle of our method to define the vibration area on an object surface. Waves propagate from the actual contact point when friction occurs. We consider that these waves spread out a rectangular domain around the actual contact point. In general, the propagating waves are attenuated in the body or prevented from spreading to the neighboring actual contact points. Therefore, the vibration of the rectangular domain around the actual contact point can be expressed by adopting an appropriate boundary condition. In this paper, we take simple support (SS) by several asperities as a boundary condition on an object surface. Given a vibration area, let S denote its rectangular domain as follows:

$$S = \left\{ (x, y, z) \;\middle|\; -\frac{a}{2} \le x \le \frac{a}{2},\ -\frac{b}{2} \le y \le \frac{b}{2},\ -\frac{h}{2} \le z \le \frac{h}{2} \right\} \tag{16}$$

where a and b are lengths of each side which is parallel to X or Y-axis. Then, the deformation (displacement w_{mn} and natural angular frequency ω_{mn}) of the rectangle domain can be described analytically by following equations:

$$w_{mn} = A \sin \frac{m\pi \left(x + \frac{a}{2}\right)}{a} \times \sin \frac{n\pi \left(y + \frac{b}{2}\right)}{b} \mathrm{e}^{-R + i\omega_{mn} t} \tag{17}$$

$$\omega_{mn} = \pi^2 \left\{ \left(\frac{m}{a}\right)^2 + \left(\frac{n}{b}\right)^2 \right\} \sqrt{\frac{Eh^3}{12\rho(1-\nu^2)}} \tag{18}$$

where A is the amplitude, m and n are the mode orders, R is the attenuation coefficient, E is Young's modulus, h is the thickness of domain S, ρ is the density per unit volume, and ν is Poisson's ratio (see Appendix A).

4.4. Sound Synthesis

The wave equation with sound sources is generally solved to analyze sound propagation in air. These equations have high computational cost due to the complex boundary conditions. In our case, a rectangle sound source can be approximated by a point sound source, because a and b (sides of the rectangle) are sufficiently small compared with the distance $|\mathbf{r}|$ between the actual contact point and the observation point. Therefore, we take the limit of $a, b \to 0$ to approximate a plane sound source with a point sound source. Then, the spatial distribution of the sound pressure $p(r, t)$, where r is the position and t is the time, is denoted as

$$p(r, t) = i\rho c V_0 \frac{k}{4\pi r} \mathrm{e}^{-ikr} \tag{19}$$

where i is the imaginary unit, ρ is the air density, c is the acoustic velocity, V_0 is the vibration velocity of the object surface, and k is

the wave number (see Appendix B). The vibration velocity V_0 can be expressed as

$$V_0 = iA\omega_{mn}\alpha_{mn}\mathrm{e}^{i\omega_{mn}t} \tag{20}$$

where

$$\alpha_{mn} = \begin{cases} 1 & m+n \equiv 0 \pmod 2 \\ -1 & m+n \equiv 1 \pmod 2 \end{cases}. \tag{21}$$

Finally, we synthesize the friction sounds caused by the vibration of each actual contact point at the observation point. Since the sound waves are independent, the synthesized sound at the observation point can be expressed as a linear sum of the sound made by each actual contact point. Therefore, the synthesized sound can be written as

$$sound = \sum_i p_i(r_i, t) \tag{22}$$

where p_i is the sound pressure of i-th vertex under friction.

5. RESULTS

We show the parameters that we use at the time of physical simulation in table 1. In the simulation, we utilize literature values [43, 44] in terms of shear modulus E, Poisson ratio ν and density par unit area ρ. The execution environment when simulating is CPU: Intel(R) core(TM) i7 CPU 2.93GHz, GPU: NVIDIA GeForce GT 220, RAM: 4GB and OS: Windows 7. Also, the time step t of the physical simulation is 1/44100 [s], the refresh rate of animations is 60 [fps] and the audio sampling rate of sounds by friction is 44100 [Hz].

5.1. Examples

cloth: In our results, we synthesize friction sounds in the case of pulling a cloth (cotton) over the sphere (see Fig. 6 and Fig. 7). We only change the velocity of a cloth in cloth1 and cloth 2. Then, our method can generate a friction sound matched to its speed in each case. Looking at the figures, there are differences between cloth 1 and 2. In particular, the results show that (i) fluctuating power of the sound denotes stick-slip and (ii) friction phenomena lead to various consequences on each frame.
metal: In this result, we generate the friction sounds of metal (cooper) sliding on the floor (see Fig. 8). As a result, we succeed to create a friction sound of the metal. The spectrum shows natural frequency of a copper on 0.31 [s] and 0.54 [s], which is caused by a picking action.

In this study, we propose the examples - a cloth pulled over the sphere and a copper sliding on the floor. In particular, the results synthesizing friction sounds for clothes are the first illustrations. In addition, our proposed method is able to manage metal like materials such as a copper. In each case, our method can synthesize a friction sound as an actual sound. In our method, we focus on the only the friction sounds. However, our method can be used in combination with other methods owing to the postulation that object surface vibrates independently, and expected to bring about sounds improving effect of correcting.

6. CONCLUSION

In this study, we presented a novel method to generate friction sounds that do not depend on the material body. The method involves physical simulation of friction on the basis of the adhesion theory. We synthesized friction sounds and confirmed that clear differences in tone appear by varying the parameters. As future works, synthesis of friction sounds with high quality in complicated scenes and body shapes is important. In particular, we would like to consider the transfer of sound waves between the object and the observation point to reflect the spatial properties affecting the sound, such as reflection, refraction, and diffraction. Further, we want to evaluate the similarity between the synthesized sounds and the actual sounds. In addition, we want to parallelize the calculations using GPUs for each actual contact point to speed up the synthesis.

7. ACKNOWLEDGMENTS

This work was supported by JST ACCEL Grant Number JPMJAC1602, Japan.

8. REFERENCES

[1] Kees Van Den Doel, Paul G Kry, and Dinesh K Pai, "Foleyautomatic: physically-based sound effects for interactive simulation and animation," in *Proceedings of the 28th annual conference on Computer graphics and interactive techniques*. ACM, 2001, pp. 537–544.

[2] Zhimin Ren, Hengchin Yeh, and Ming C Lin, "Synthesizing contact sounds between textured models," in *Virtual Reality Conference (VR), 2010 IEEE*. IEEE, 2010, pp. 139–146.

[3] Steven S An, Doug L James, and Steve Marschner, "Motion-driven concatenative synthesis of cloth sounds," *ACM Transactions on Graphics (TOG)*, vol. 31, no. 4, pp. 102–111, 2012.

[4] Camille Schreck, Damien Rohmer, Doug James, Stefanie Hahmann, and Marie-Paule Cani, "Real-time sound synthesis for paper material based on geometric analysis," in *Eurographics/ACM SIGGRAPH Symposium on Computer Animation (2016)*, 2016.

[5] Andrew Owens, Phillip Isola, Josh McDermott, Antonio Torralba, Edward H Adelson, and William T Freeman, "Visually indicated sounds," in *Proceedings of the IEEE Conference on Computer Vision and Pattern Recognition*, 2016, pp. 2405–2413.

[6] Lieng-Huang Lee, *Fundamentals of adhesion*, Springer Science & Business Media, 2013.

[7] Matthias Müller, Bruno Heidelberger, Marcus Hennix, and John Ratcliff, "Position based dynamics," *Journal of Visual Communication and Image Representation*, vol. 18, no. 2, pp. 109–118, 2007.

[8] JT Oden and JAC Martins, "Models and computational methods for dynamic friction phenomena," *Computer methods in applied mechanics and engineering*, vol. 52, no. 1, pp. 527–634, 1985.

[9] JAC Martins, JT Oden, and FMF Simoes, "A study of static and kinetic friction," *International Journal of Engineering Science*, vol. 28, no. 1, pp. 29–92, 1990.

[10] Yu A Karpenko and Adnan Akay, "A numerical model of friction between rough surfaces," *Tribology International*, vol. 34, no. 8, pp. 531–545, 2001.

Table 1: *List of conditions at the time of the physical simulation*

	Shear modulus E [GPa]	Poison ratio ν	Density ρ [kg/m^2]	a, b [m]	Dispersion σ^2	Vertex	Time [min]
cloth1	928.7	0.85	1.54×10^1	5.0×10^{-4}	1.0×10^{-12}	900	31
cloth2	928.7	0.85	1.54×10^1	5.0×10^{-4}	1.0×10^{-12}	900	59
copper	129.8	0.343	8.94	1.0×10^{-8}	1.0×10^{-7}	242	72

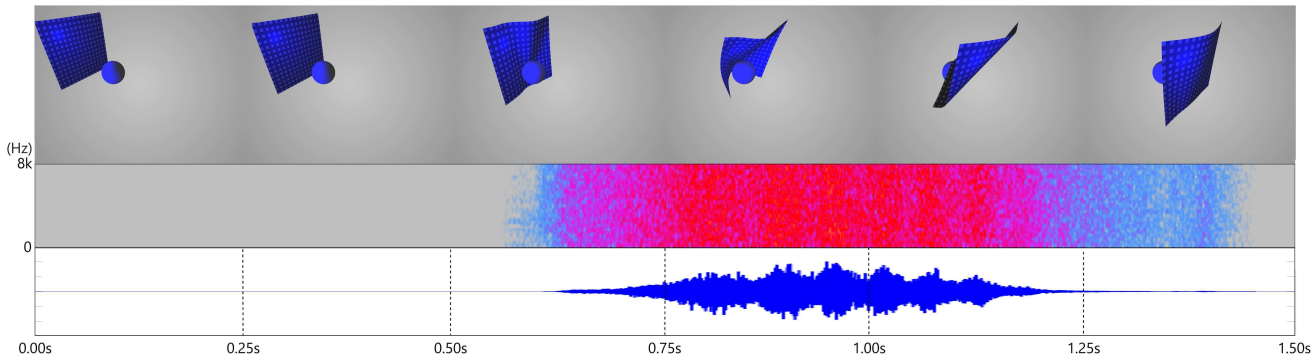

Figure 6: *Key frames and sound waveform of a cloth (cotton). In this example, pull a cloth toward the front and slide it over the sphere.*

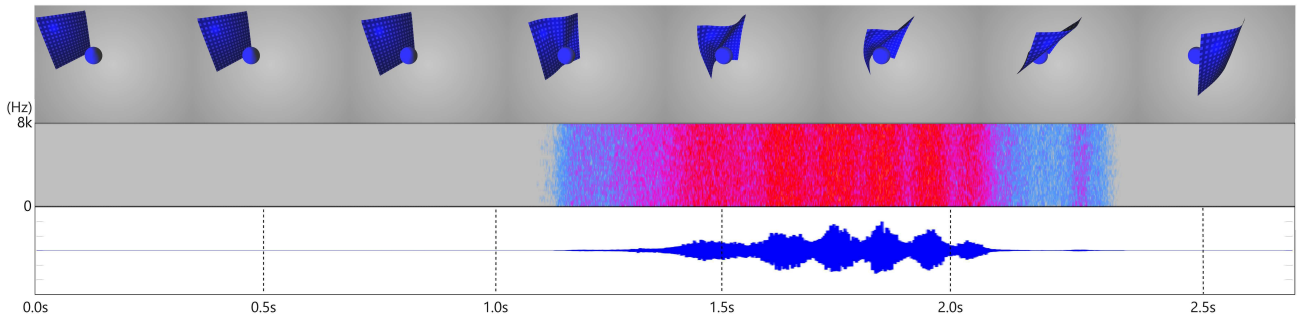

Figure 7: *Key frames and sound waveform of a cloth (cotton). In this example, change the velocity of pulling a cloth (× 1/2).*

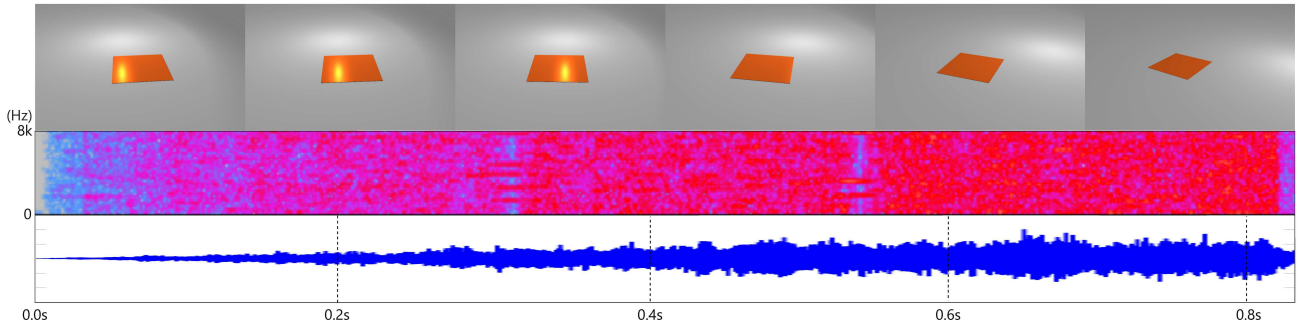

Figure 8: *Key frames and sound waveform of a metal (copper). In this example, slide a copper on the floor.*

[11] Federico Avanzini, Stefania Serafin, and Davide Rocchesso, "Modeling interactions between rubbed dry surfaces using an elasto-plastic friction model," in *Proc. DAFX*, 2002.

[12] Charlotte Desvages and Stefan Bilbao, "Two-polarisation finite difference model of bowed strings with nonlinear contact and friction forces," in *Int. Conference on Digital Audio Effects (DAFx-15)*, 2015.

[13] Adnan Akay, "Acoustics of friction," *The Journal of the Acoustical Society of America*, vol. 111, no. 4, pp. 1525–1548, 2002.

[14] Tapio Takala and James Hahn, "Sound rendering," in *ACM*

SIGGRAPH Computer Graphics. ACM, 1992, vol. 26, pp. 211–220.

[15] William W Gaver, "Synthesizing auditory icons," in *Proceedings of the INTERACT'93 and CHI'93 conference on Human factors in computing systems*. ACM, 1993, pp. 228–235.

[16] Kees van de Doel and Dinesh K Pai, "Synthesis of shape dependent sounds with physical modeling," 1996.

[17] Kees van den Doel and Dinesh K Pai, "The sounds of physical shapes," *Presence: Teleoperators and Virtual Environments*, vol. 7, no. 4, pp. 382–395, 1998.

[18] Kevin Karplus and Alex Strong, "Digital synthesis of plucked-string and drum timbres," *Computer Music Journal*, vol. 7, no. 2, pp. 43–55, 1983.

[19] Perry R Cook, *Real sound synthesis for interactive applications*, CRC Press, 2002.

[20] Stefan Bilbao, *Numerical sound synthesis: finite difference schemes and simulation in musical acoustics*, John Wiley & Sons, 2009.

[21] Andrew Allen and Nikunj Raghuvanshi, "Aerophones in flatland: interactive wave simulation of wind instruments," *ACM Transactions on Graphics (TOG)*, vol. 34, no. 4, pp. 134, 2015.

[22] James F Director-O'Brien, "Synthesizing sounds from physically based motion," in *ACM SIGGRAPH 2001 video review on Animation theater program*. ACM, 2001, pp. 59–66.

[23] James F O'Brien, Chen Shen, and Christine M Gatchalian, "Synthesizing sounds from rigid-body simulations," in *Proceedings of the 2002 ACM SIGGRAPH/Eurographics symposium on Computer animation*. ACM, 2002, pp. 175–181.

[24] Dinesh K Pai, Kees van den Doel, Doug L James, Jochen Lang, John E Lloyd, Joshua L Richmond, and Som H Yau, "Scanning physical interaction behavior of 3d objects," in *Proceedings of the 28th annual conference on Computer graphics and interactive techniques*. ACM, 2001, pp. 87–96.

[25] Cynthia Bruyns, "Modal synthesis for arbitrarily shaped objects," *Computer Music Journal*, vol. 30, no. 3, pp. 22–37, 2006.

[26] Nobuyuki Umetani, Jun Mitani, and Takeo Igarashi, "Designing custom-made metallophone with concurrent eigenanalysis.," in *NIME*. Citeseer, 2010, vol. 10, pp. 26–30.

[27] Gaurav Bharaj, David IW Levin, James Tompkin, Yun Fei, Hanspeter Pfister, Wojciech Matusik, and Changxi Zheng, "Computational design of metallophone contact sounds," *ACM Transactions on Graphics (TOG)*, vol. 34, no. 6, pp. 223, 2015.

[28] Nikunj Raghuvanshi and Ming C Lin, "Interactive sound synthesis for large scale environments," in *Proceedings of the 2006 symposium on Interactive 3D graphics and games*. ACM, 2006, pp. 101–108.

[29] Doug L James, Jernej Barbič, and Dinesh K Pai, "Precomputed acoustic transfer: output-sensitive, accurate sound generation for geometrically complex vibration sources," in *ACM Transactions on Graphics (TOG)*. ACM, 2006, vol. 25, pp. 987–995.

[30] Nicolas Bonneel, George Drettakis, Nicolas Tsingos, Isabelle Viaud-Delmon, and Doug James, "Fast modal sounds with scalable frequency-domain synthesis," in *ACM Transactions on Graphics (TOG)*. ACM, 2008, vol. 27, pp. 24–32.

[31] Jeffrey N Chadwick, Steven S An, and Doug L James, "Harmonic shells: a practical nonlinear sound model for near-rigid thin shells," in *ACM Transactions on Graphics (TOG)*. ACM, 2009, vol. 28, pp. 119–128.

[32] Changxi Zheng and Doug L James, "Rigid-body fracture sound with precomputed soundbanks," in *ACM Transactions on Graphics (TOG)*. ACM, 2010, vol. 29, pp. 69–81.

[33] Changxi Zheng and Doug L James, "Toward high-quality modal contact sound," *ACM Transactions on Graphics (TOG)*, vol. 30, no. 4, pp. 38–49, 2011.

[34] Jeffrey N Chadwick, Changxi Zheng, and Doug L James, "Precomputed acceleration noise for improved rigid-body sound," *ACM Transactions on Graphics (TOG)*, vol. 31, no. 4, pp. 103–111, 2012.

[35] Timothy R Langlois, Steven S An, Kelvin K Jin, and Doug L James, "Eigenmode compression for modal sound models," *ACM Transactions on Graphics (TOG)*, vol. 33, no. 4, pp. 40–48, 2014.

[36] Gabriel Cirio, Dingzeyu Li, Eitan Grinspun, Miguel A Otaduy, and Changxi Zheng, "Crumpling sound synthesis," *ACM Transactions on Graphics (TOG)*, vol. 35, no. 6, pp. 181, 2016.

[37] Matthias Rath, "Energy-stable modelling of contacting modal objects with piece-wise linear interaction force," *DAFx-08, Espoo, Finland*, 2008.

[38] Stefano Papetti, Federico Avanzini, and Davide Rocchesso, "Energy and accuracy issues in numerical simulations of a non-linear impact model," in *Proc. Of the 12th Int. Conference on Digital Audio Effects*, 2009.

[39] Arthur W Leissa, "Vibration of plates," Tech. Rep., DTIC Document, 1969.

[40] Miguel C Junger and David Feit, *Sound, structures, and their interaction*, vol. 225, MIT press Cambridge, MA, 1986.

[41] Xavier Provot, "Deformation constraints in a mass-spring model to describe rigid cloth behaviour," in *Graphics interface*. Canadian Information Processing Society, 1995, pp. 147–147.

[42] Matthias Müller, Bruno Heidelberger, Matthias Teschner, and Markus Gross, "Meshless deformations based on shape matching," in *ACM Transactions on Graphics (TOG)*. ACM, 2005, vol. 24, pp. 471–478.

[43] Shigeta Fujimoto, "Modulus of rigidity as fiber properties," *Textile Engineering*, vol. 22, no. 5, pp. 369–376, 1969.

[44] National Astronomical Observatory of Japan, Ed., *Chronological Science Tables 2016 A.D.*, Maruzen, 2015.

A. VIBRATION OF PLATE

Suppose a micro rectangle is an elastic isotropic plate and there are no normal forces N_i, inplane shearing forces N_{ij} and external

forces q. Then, displacement $w(\vec{x},t)$ of the plate is expressed in the following equation:

$$D\nabla^4 w + \rho\frac{\partial^2 w}{\partial t^2} = 0 \tag{23}$$

where D is flexural rigidity defined as follow,

$$D = \frac{Eh^3}{12(1-\nu^2)} \tag{24}$$

where E is Young's modulus, h is the thickness of plate, and ν is Poisson's rate. A general solution of the expression (23) is given by the following formula:

$$w = W(x,y)e^{i\omega t} \tag{25}$$

$$W(x,y) = X(x)Y(y) \tag{26}$$

where ω is angular frequency. And, $W(x,y)$ is calculated from the following formula:

$$\left(\nabla^4 - \frac{\rho\omega^2}{D}\right)W(x,y) = 0 \tag{27}$$

Then, define the domain S of a plate as follows:

$$S = \left\{(x,y,z) \;\middle|\; 0 \le x \le a,\ 0 \le y \le b,\ -\frac{h}{2} \le z \le \frac{h}{2}\right\} \tag{28}$$

Solve equation (27) assuming that boundary conditions of a plate are Simple Support for four sides under the following conditions:

$$w = 0, M_x = 0 \quad (for\ \ x = 0, a) \tag{29}$$

$$w = 0, M_y = 0 \quad (for\ \ y = 0, b) \tag{30}$$

where M_i is bending moment. With normal stress σ_i, bending moment M_i is expressed by the following formula.

$$M_i = \int_{-h/2}^{h/2} \sigma_i z dz \quad (for\ \ i = x, y) \tag{31}$$

Finally, we obtain the equations which is indicated in Section 4.3 as below.

$$W(x,y) = A\ sin\ \frac{m\pi x}{a}\ sin\ \frac{n\pi y}{b} \tag{32}$$

$$\omega_{mn} = \sqrt{\frac{D}{\rho}}\left\{\left(\frac{m\pi}{a}\right)^2 + \left(\frac{n\pi}{b}\right)^2\right\} \tag{33}$$

B. POINT SOUND SOURCE ANALYSIS

Let convert a wave equation into polar coordinates system from Descartes coordinate system to think about the spread of the sounds from a point sound source as follow:

$$\nabla^2\phi(r,\theta,\varphi) - \frac{1}{c^2}\frac{\partial^2\phi(r,\theta,\varphi)}{\partial t^2} = 0 \tag{34}$$

where

$$\begin{aligned}\nabla^2 &= \frac{1}{r^2}\frac{\partial}{\partial r}\left(r^2\frac{\partial}{\partial r}\right) \\ &\quad + \frac{1}{r^2 sin\,\theta}\frac{\partial}{\partial\theta}\left(sin\,\theta\frac{\partial}{\partial\theta}\right) \\ &\quad + \frac{1}{r^2 sin^2\,\theta}\frac{\partial^2}{\partial\varphi^2}\end{aligned} \tag{35}$$

The sounds from a point sound source spread symmetrically and spherically. Therefore, we should only think about a component of radius direction. Then, we obtain the general solution of a wave equation in the polar coordinates system as below:

$$\phi(r) = \frac{A}{r}e^{i(\omega t - kr)} \tag{36}$$

where A is the constant. As mentioned in Section 3.2, acoustic pressure $p(r,t)$ and particle velocity $\mathbf{u}(r,t)$ are made use of a variable in acoustics as follows:

$$\left(\nabla^2 - \frac{1}{c^2}\frac{\partial^2}{\partial t^2}\right)p(r,t) = 0 \tag{37}$$

$$\left(\nabla^2 - \frac{1}{c^2}\frac{\partial^2}{\partial t^2}\right)\mathbf{u}(r,t) = 0 \tag{38}$$

where c is the acoustic velocity. Now, to derive the expression (19) using a general solution (36), suppose that the acoustic pressure $p(r,t)$ is as follow:

$$p(r,t) = \frac{A}{r}e^{i(\omega t - kr)} \tag{39}$$

Then, particle velocity $\mathbf{u}(r,t)$ is indicated by the following formula:

$$\begin{aligned}\mathbf{u}(r,t) &= -\frac{1}{\rho}\int dt\frac{\partial p}{\partial r} \\ &= -\frac{A}{\rho}\int dt\frac{\partial}{\partial r}\left\{\frac{1}{r}e^{i\omega\left(t-\frac{r}{c}\right)}\right\} \\ &= \frac{A}{\rho c}\frac{1}{r}\left(1+\frac{1}{ikr}\right)e^{i(\omega t - kr)}\end{aligned} \tag{40}$$

From the initial condition, the constant A is given by the following:

$$\begin{aligned}\mathbf{u}(a,0) &= U_0 = \frac{A}{\rho c}\frac{1}{a}\left(1+\frac{1}{ika}\right)e^{-ika} \\ A &= \rho a c U_0\frac{ika}{1+ika}e^{ika}\end{aligned} \tag{41}$$

Finally, to take the limit of $a, b \to 0$, we can get the acoustic pressure $p(r,t)$ of a point sound source as below:

$$\begin{aligned}p(r,t) &= \frac{A}{r}e^{i(\omega t - kr)} \\ &= \frac{\rho c U_0}{4\pi}\frac{ika}{1+ika}e^{i(\omega t - k(r-a))} \\ &\to i\rho c V_0\frac{k}{4\pi r}e^{i(\omega t - kr)}\end{aligned} \tag{42}$$

where V_0 is the oscillate speed as follow.

$$U_0 = 4\pi a^2 V_0 \tag{43}$$